Inorganic Gas-Phase Reactions of the Nitrate Radical: $I_2 + NO_3$ and $I + NO_3$

R. M. Chambers, A. C. Heard,† and R. P. Wayne*

Physical Chemistry Laboratory, South Parks Road, Oxford, OX1 3QZ, UK *(Received: October 11, 1991; In Final Form: December 30, 1991)*

A low-pressure discharge-flow technique, with various optical detection methods, has been used to determine, for the first time, bimolecular rate coefficients for the reactions between I_2 and NO_3, $k_1 = (1.5 \pm 0.5) \times 10^{-12}$ cm^3 molecule^{-1} s^{-1}, and I and NO_3, $k_2 = (4.5 \pm 1.9) \times 10^{-10}$ cm^3 molecule^{-1} s^{-1}. No temperature dependence over the range 292–423 K, or pressure dependence from 1.2 to 4.7 Torr, was observed for the reaction $I_2 + NO_3$. A heterogeneous generation of I atoms was observed in the $I + NO_3$ reaction system which was interpreted as evidence for the reaction of IO at the surface of the flow reactor to form a higher oxide of iodine and iodine atoms. The rate coefficient for reaction of IO at the walls to form I was found to be 25–45 s^{-1}. An upper limit for the heat of formation of $IONO_2$ of 21 ± 3 kJ mol^{-1} was also derived.

1. Introduction

The importance of NO_3 in the troposphere has only been recognized for the past 20 years or so, and it is now known that the radical controls the concentration of odd nitrogen compounds (mainly NO, NO_2, N_2O_5, HNO_3, $CH_3CO{\cdot}O_2NO_2$) at night. It also acts as a source of nitric acid, oxidizes a range of organic species, produces peroxy and hydroxy radicals, and yields nitrate products that may act as temporary reservoirs of oxides of nitrogen. The physical and chemical behavior of NO_3, with special emphasis on atmospheric processes, has recently been reviewed by Wayne et al.,[1] and the published kinetic data for reactions between NO_3 and organic compounds have been critically evaluated by Atkinson.[2] The only identified natural sources of iodine are CH_3I and I_2 from seawater.[3,4] However, iodine is also released to the atmosphere as a result of industrial activity. In particular, radioactive iodine (^{129}I), formed as a fission product of uranium fuels, is a potentially harmful airborne emission from nuclear power installations.[5] The chemistry of iodine species in the atmosphere would therefore be one of the dominant processes determining the rate of deposition and hence the lifetime in the atmosphere of ^{129}I after a nuclear accident. The atmospheric chemistry of iodine-containing compounds is very different from that of the chlorine- and bromine-containing substances. All species are short-lived during the daytime as they are readily photolyzed by wavelengths in the visible region, and all chemical conversions involving iodine occur in the troposphere. Possible reactions of CH_3I or I_2 with other atmospheric species have been little studied because photolysis occurs for wavelengths less than $\lambda = 400$ nm or $\lambda = 500$ nm, respectively, and photodissociation is expected to be the dominant loss process. Brown et al.[6] found that reaction of CH_3I with the OH radical could account for only 2% of the overall loss in CH_3I compared with the case of photolysis. Gaseous iodine species are removed rapidly at the ocean surface by attachment to particles.[7] However, Zafiriou[8] calculates that over 95% of molecular iodine undergoes photolysis and less than 5% is lost heterogeneously. Consequently, CH_3I has been considered in tropospheric chemistry mainly as a source of atomic I.[9-11]

The central part of the present study is concerned with the reactions between NO_3 and molecular and atomic iodine

$$I_2 + NO_3 \rightarrow \text{products} \quad (1)$$

$$I + NO_3 \rightarrow IO + NO_2 \quad (2)$$

Neither of these two reactions had been observed before our experiments were conducted, and still no reaction, other than (1), between NO_3 and a homonuclear diatomic molecule is known in the gas phase. There are several potential channels for reaction 1, but all are highly endothermic with the possible exception of the process

$$I_2 + NO_3 \rightarrow I + IONO_2 \quad (1a)$$

We shall show, in our discussion, that the rapidity of reaction 1 enables us to place a new upper limit on the heat of formation of $IONO_2$.

The reactions

$$X + NO_3 \rightarrow XO + NO_2 \quad (3)$$

where X = F, Cl, or Br, have been studied previously[12-20] and have been found to occur rapidly [observed bimolecular rate constants range from 7.6×10^{-11} cm^3 molecule^{-1} s^{-1} for X = Cl[12] to 1.6×10^{-11} cm^3 molecule^{-1} s^{-1} for X = Br[20]]. There has been only one other reported study that is relevant to the reaction between I and NO_3. Lançar et al.[21] state that they *failed* to see any reaction between I and NO_3, although no details of their investigation of that particular reaction are given. In contrast, the bimolecular rate coefficient observed in our studies suggests that almost every gas-phase collision of an iodine atom and a nitrate radical results in a chemical transformation.

In this work a low-pressure discharge-flow technique was used to measure the rates of reactions 1 and 2. Concentrations of I_2, I, and NO_3 were monitored simultaneously using laser-induced fluorescence, atomic resonance fluorescence, and optical absorption, respectively. The concentrations of NO_3 used were much greater than either $[I_2]$ or [I], so that during a kinetic experiment $[NO_3]$ remained constant, thus simplifying the analysis of the experimental data.

† Current address: CSIRO Division of Applied Physics, PO Box 218, Lindfield NSW 2070, Australia.

(1) Wayne, R. P.; Barnes, I.; Biggs, P.; Burrows, J. P.; Canosa-Mas, C. E.; Hjorth, J.; LeBras, G.; Moortgat, G.; Perner, D.; Poulet, G.; Restelli, G.; Sidebottom, H. *Atmos. Environ.* **1991**, *25A*, 1.
(2) Atkinson, R. *J. Phys. Chem. Ref. Data* **1991**, *20*, 459.
(3) Lovelock, J. E.; Maggs, R. J.; Wade, R. J. *Nature* **1973**, *241*, 194.
(4) Garland, J. A.; Curtis, H. *J. Geophys. Res.* **1981**, *86*, 3183.
(5) Jenkin, M. E.; Cox, R. A.; Candeland, D. E. *J. Atmos. Chem.* **1985**, *2*, 359.
(6) Brown, A. C.; Canosa-Mas, C. E.; Wayne, R. P. *Atmos. Environ.* **1990**, *24A*, 361.
(7) Chamberlain, A. C.; Eggleton, A. E. J.; Megaw, W. J.; Morris, J. B. *Discuss. Faraday Soc.* **1960**, *30*, 1.
(8) Zafiriou, O. C. *J. Geophys. Res.* **1974**, *79*, 2730.
(9) Chameides, W. L.; Davies, D. D. *J. Geophys. Res.* **1980**, *85*, 7383.
(10) Chatfield, R. B.; Crutzen, P. J. *J. Geophys. Res.* **1990**, *95*, 22, 319.
(11) Jenkin, M. E. Ph.D. Thesis, University of East Anglia, 1991.
(12) Cox, R. A.; Barton, R. A.; Ljungstrom, E.; Stocker, D. W. *Chem. Phys. Lett.* **1984**, *108*, 228.
(13) Rahman, M. M.; Becker, E.; Benter, Th.; Schindler, R. N. *Ber. Bunsen-Ges. Phys. Chem.* **1988**, *92*, 91.
(14) Ravishankara, A. R.; Wine, P. H. *Chem. Phys. Lett.* **1983**, *101*, 73.
(15) Sander, S. P. *J. Phys. Chem.* **1986**, *90*, 4135.
(16) Burrows, J. P.; Wallington, T. J.; Wayne, R. P. *J. Chem. Soc., Faraday Trans. 2* **1983**, *79*, 111.
(17) Cox, R. A.; Fowles, M.; Moulton, D.; Wayne, R. P. *J. Phys. Chem.* **1987**, *91*, 3361.
(18) Mellouki, A.; LeBras, G.; Poulet, G. *J. Phys. Chem.* **1987**, *91*, 5760.
(19) Ewig, F.; Hoffman, A.; Zellner, R. Presented at the Xth International Symposium on Gas Kinetics, Swansea, United Kingdom, 1988, 24–29 July.
(20) Mellouki, A.; Poulet, G.; LeBras, G.; Singer, R.; Burrows, J. P.; Moortgat, G. K. *J. Phys. Chem.* **1989**, *93*, 8017.
(21) Lançar, I. T.; Mellouki, A.; Poulet, G. *Chem. Phys. Lett.* **1991**, *177*, 554.

0022-3654/92/2096-3321$03.00/0

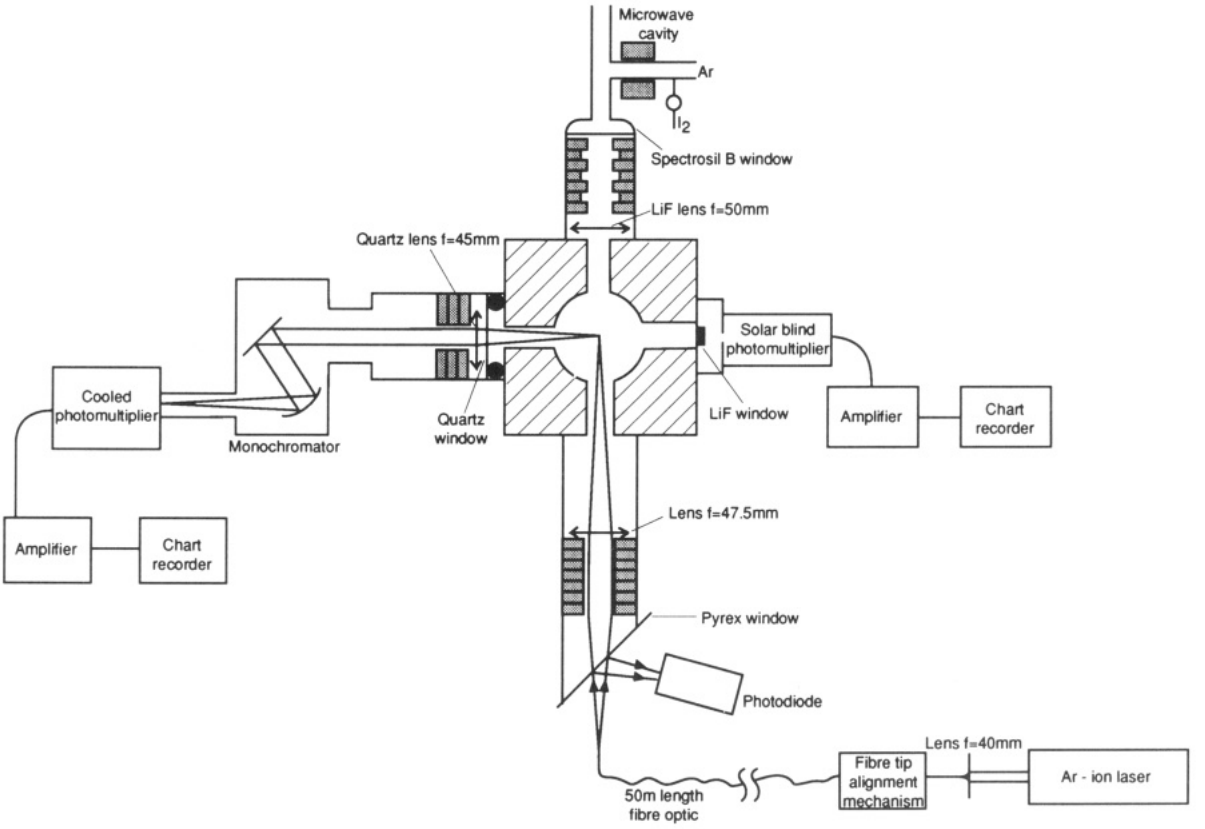

Figure 1. The fluorescence cell for detection of I_2 and I.

2. Experimental Section

A Pyrex flow tube 86.2 cm long and of 3.8 cm i.d. was pumped by a rotary pump (Edwards ISC900) of displacement 900 L h^{-1}, providing stable linear flow velocities (of helium) of between 707 and 1609 cm s^{-1} at the pressures typically used in this work (1.0–4.7 Torr). A stainless-steel observation cell and an absorption cell were situated downstream of the flow tube as shown previously.[22] The flow tube was internally coated with halocarbon wax (Halocarbon Corp., Series 15-00), in order to reduce heterogeneous losses of reactive species. Time resolution was provided by a Pyrex sliding injector, having an external diameter of 12 mm and a spray nozzle tip, through which one of the reactants was passed into the flow tube. Pressures in the flow tube were measured by a manometer containing di-*n*-butyl phthalate; this manometer was cross-checked against a capacitance manometer (10 Torr, MKS Baratron). Gases were delivered via flow meters (Jencon RS1 or capillary flow meters) and needle valves (Nupro). All flow meters were calibrated for each reactant mixture. The temperature of the flow tube was regulated over a range of 292–427 K using an electric heating tape (Hotfoil Type G1) with thermostatic controller, as described previously.[23]

NO_3 was formed by the reaction between atomic fluorine and nitric acid as outlined in ref 24. The NO_3 could be made either in the main flow tube or in the sliding injector. NO_3 was detected by optical absorption at λ = 662 nm using a tungsten–halogen lamp as a light source together with an interference filter with a band center at λ = 661.9 nm (fwhm = 4 nm, Ealing Electro-Optics Ltd.). The path length of the White cell was approximately 156 cm (corresponding to 12 passes) for much of the work presented here, although 16 passes were occasionally used (path length $\simeq$ 208 cm). The reference and sample beams were alternately chopped (Bentham Type 200, 20 Hz) and were guided to a photomultiplier (Thorn EMI 9781R, used as a photocell) via a 1-m length of bifurcated fiber optic (Schott Glass Ltd.). The signal from the photomultiplier was demodulated by a phase-sensitive detector.[24] Absolute concentrations of NO_3 were determined by chemical titration with a known amount of NO.[24] NO_3 concentrations in the range (0.8–25) $\times$ 10^{12} molecules cm^{-3} were used. The absolute sensitivity for NO_3 measurement was about 10^{11} molecules cm^{-3} for a signal-to-noise ratio of unity with a 10-s integration time.

A schematic diagram of the fluorescence cell used to detect I_2 and I in the flow system is shown in Figure 1. A stable I_2 fluorescence signal was achieved with a steady flow of He through a reservoir of iodine crystals. The temperature of the iodine reservoir was regulated using an ethanediol/solid CO_2 slush bath. Iodine could be admitted to the main flow tube or via the sliding injector with the iodine reservoir attached to the sliding injector itself. The I_2 was monitored by the technique of laser-induced fluorescence (LIF). Monochromatic light (λ = 514.9 nm) from an Ar ion laser (Coherent Innova 70) was directed via a 50-m length of fiber optic (York VSOP, SM450) custom optimized for the transmission of monochromatic radiation at a wavelength of 488 nm. The diameter of the fiber core was 2.5 μm so that aligning it with respect to the laser beam was critical. The intensity of the laser beam was attenuated by over 2 orders of magnitude from ca. 1.3 W to ca. 10 mW (210 Power Meter, Coherent Radiation) by the fiber optic. The relative laser intensity was monitored continuously by a photodiode (BPX65) placed so as to detect light from the first reflection at the lower window of the baffled arm in which a focusing lens is placed (Figure 1). The focused radiation excites the ground electronic state of $I_2(^1\Sigma_g^+)$ to $I_2(^3\Pi_{0_u})$. The emitted radiation passes through a monochromator (Bausch and Lomb high-intensity grating monochromator, Type 33-86-26-07) and is detected at λ = 539 nm (fwhm = 17 nm) by a cooled photomultiplier (Thorn EMI, Type 9757QB, –40 °C). The iodine fluorescence signal was calibrated using a known concentration of I_2 in He. The LIF intensity was directly proportional both to $[I_2]$ and to the laser intensity. The linear dependence on laser power shows that the electronic transition is not saturated[25] under our experimental conditions. The absolute

(22) Boodaghians, R. B.; Canosa-Mas, C. E.; Carpenter, P.; Wayne, R. P. *J. Chem. Soc., Faraday Trans. 2* **1988**, *84*, 931.
(23) Brown, A. C.; Canosa-Mas, C. E.; Parr, A. D.; Wayne, R. P. *Atmos. Environ.* **1990**, *24A*, 2499.
(24) Canosa-Mas, C. E.; Fowles, M.; Houghton, P. J.; Wayne, R. P. *J. Chem. Soc., Faraday Trans. 2* **1987**, *83*, 1465.

sensitivity for I_2 measurement was about 10^{10} molecules cm^{-3} for a signal-to-noise ratio of unity with a 10-s integration time.

Iodine atoms were made in two ways: first, directly by exciting a microwave discharge (50 W) in a dilute mixture of I_2 in helium, and second, by the rapid reaction[26] between oxygen atoms and molecular iodine

$$O + I_2 \rightarrow I + IO \quad (4)$$

the O atoms being generated in a microwave discharge (40 W) through a dilute ($\simeq$10%) flow of oxygen in helium. The I atoms were detected using atomic resonance fluorescence, with exciting radiation being obtained from a lamp in which a flow of I_2/Ar was subject to a microwave discharge (50 W). A reservoir of iodine crystals at room temperature was situated just before the microwave cavity, and the I_2 was allowed to sublime into the flow of Ar. A window of Spectrosil B (UQG Ltd.) combined with a solar blind photomultiplier (Hamamatsu R1459) was used to provide a band-pass region of $170 < \lambda < 200$ nm for observation of I atom emissions. Optimum operating conditions were with the I_2 reservoir at ambient temperature and an Ar pressure of about 0.2 Torr. The lamp and detection system were attached to the fluorescence cell as shown in Figure 1, the light from the I atom lamp being focused (LiF lens, BDH Crystran) into the center of the cell. A first approximation to the sensitivity of the arrangement described for the detection of I was obtained by creating I atoms in the flow tube using a microwave discharge on a flow of I_2/He and monitoring simultaneously the decrease in $[I_2]$ and the increase in I fluorescence signal. The maximum concentration of I possible is twice the concentration of iodine molecules lost. A sensitivity of $>10^9$ molecules cm^{-3} for a signal-to-noise ratio of unity and a 10-s integration time was estimated by this procedure.

Materials. Helium (BOC, commercial grade) was passed over red-hot copper turnings to remove traces of O_2 and H_2, through molecular sieve and P_2O_5 drying towers, and finally through cold traps (77 K) on both high- and low-pressure sides of the main needle valve. Nitric oxide (BDH Ltd.) was purified by a rigorous trap-to-trap distillation procedure (77 K) until the remaining solid was white. HNO_3 (BDH Ltd., Aristar, 70%) and H_2SO_4 (Fisons, 98%) were combined in a 1:2 mixture which was frozen down and degassed to remove NO_2 impurity prior to use. F_2 (5% in He, BOC Special Gases) was used as received. I_2 (BDH, Ltd., >99.9%) was degassed by repeated "freeze–pump–warm-up" cycles.

3. Results

3.1. Reaction between NO_3 and I_2. *3.1.1. Kinetics.* The concentrations of nitrate radical and molecular iodine were monitored simultaneously. NO_3 was added either through the sliding injector or through the side arm of the main flow tube. In experiments in which the I_2 was admitted to the flow reactor via the movable inlet, $[I_2]$ was invariant with injector position in the absence of NO_3, so that there appears to be no detectable heterogeneous loss of I_2

$$I_2 + \text{wall} \rightarrow \text{products} \quad (5)$$

$$k_5 \leq 0.5\ s^{-1}$$

A time-dependent decay of I_2 in the presence of NO_3 was observed, and this decay is interpreted as evidence for the occurrence of the reaction

$$I_2 + NO_3 \rightarrow \text{products} \quad (1)$$

The iodine concentration was measured with ($[I_2]$) and without ($[I_2]_0$) NO_3 added to the flow tube for each position of the sliding injector. If NO_3 is in large excess over I_2, the decay of I_2 is expected to be pseudo-first-order, so that $\ln\{[I_2]_0/[I_2]\}$ will be a linear function of contact time. A typical pseudo-first-order plot is shown in Figure 2. The slope of each graph, k_1' ($k_1' = k_1[NO_3]$), was then plotted against the concentration of NO_3 to give the second-order rate constant. The experimental conditions for each kinetic run at ambient temperature are summarized in Table I. Data from Table I (T = 292–297 K) are shown in Figure 3. The slope of the second-order plot gives $k_1(295\ K) = (1.5 \pm 0.1) \times 10^{-12}$ cm^3 $molecule^{-1}$ s^{-1}. The data cover the pressure range 1.2–4.7 Torr, and it appears that there is no pressure dependence for the reaction over this range. We also studied the reaction at different temperatures of the flow tube, and the results are shown in Table II. As can be seen from Tables I and II, the rate coefficient for the reaction between I_2 and NO_3 is apparently independent of temperature over the range 292–427 K.

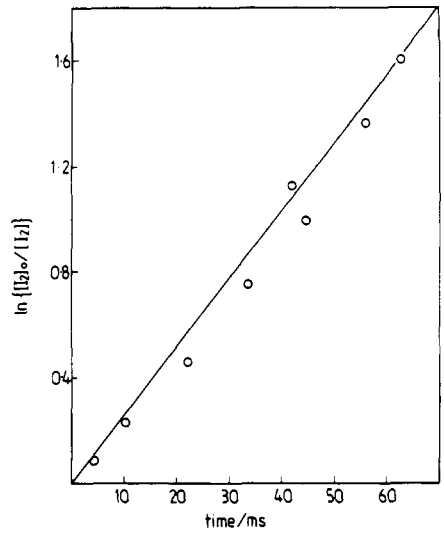

Figure 2. Pseudo-first-order plot for the reaction $I_2 + NO_3$. T = 292 K, P_{ft} = 1.9 Torr, $[I_2] = 2.4 \times 10^{11}$ molecules cm^{-3}, $[NO_3] = 15.7 \times 10^{12}$ molecules cm^{-3}.

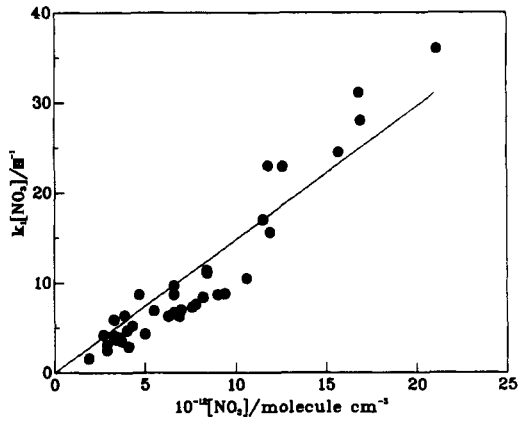

Figure 3. Second-order plot for the reaction $I_2 + NO_3$. T = 292–297 K, P_{ft} = 1.2–4.7 Torr.

Technical problems with the calibrations for absolute $[I_2]$ at elevated temperatures mean that the values of $[I_2]$ given in Table II are lower limits. Nevertheless, there was never any evidence in our experiments of deviation from pseudo-first-order behavior. The errors in the rate coefficients quoted in Tables I and II are the 95% confidence limits obtained from a linear least-squares fit to the data. The error in the determination of $[NO_3]$ is about 26%. Radial and axial diffusion will affect the measurement of k_1. For conditions in which wall losses are low and diffusion is rapid compared with reaction, the correction factor $f = k_{true}/k_{obs}$ can be written[27] in the simplified form

$$f = 1 + \frac{k_{obs}D}{\bar{v}^2} + \frac{k_{obs}r^2}{48D} \quad (i)$$

$\bar{v}$ is the linear flow velocity, and r is the radius of the flow reactor.

(25) Hancock, G. *J. Chem. Soc., Faraday Trans. 2* **1988**, *84*, 429.
(26) Ray, G. W.; Watson, R. T. *J. Phys. Chem.* **1981**, *85*, 2955.
(27) Keyser, L. F. *J. Phys. Chem.* **1984**, *88*, 4750.

TABLE I: Experimental Data for the Reaction $I_2 + NO_3$ at Ambient Temperature

T, K	P_{ft}, Torr	$\bar{v}$, cm s^{-1}	$10^{-11}[I_2]$, molecules cm^{-3}	$10^{-12}[NO_3]$, molecules cm^{-3}	k_1', s^{-1}	$10^{12}k_1$, cm^3 molecule^{-1} s^{-1}
292	2.0	1306	0.7	6.6	6.7	
		1268	1.9	7.6	7.3	
		1314	0.7	2.9	2.5	
		767	0.6	9.0	8.7	
		767	0.5	5.0	4.3	
		767	0.8	6.9	6.3	
		767	0.7	1.9	1.6	
296	2.1	707	1.4	10.6	10.5	
		707	1.2	6.3	6.3	
		707	1.0	9.4	8.8	
296.5	2.0	814	4.7	7.8	7.6	
		810	6.0	3.7	3.5	
295.5	2.0	753		8.2	8.4	
		753		3.6	3.9	
295	1.3	1292		2.7	4.2	1.5 ± 0.1
		1230	8.8	4.0	4.7	
	1.2	1298	9.8	5.5	6.9	
		1298	8.3	6.6	8.7	
		849	6.5	7.0	7.0	
		846	6.1	4.3	5.2	
		846	3.6	3.3	4.1	
294	1.4	1143	2.0	8.4	11.5	
292	4.2	793	1.0	2.9	3.1	
		793	0.8	3.3	5.6	
		793	1.8	4.7	8.7	
	4.5	748	2.9	3.4	3.7	
		748	4.3	4.1	2.9	
295	4.7	1051	4.0	11.8	23.0	
		1051	3.4	11.5	17.0	
		1048	4.9	8.4	11.1	
297	2.1	1312	1.4	3.9	6.4	
		1311	4.6	11.9	15.6	
	1.9	843	3	6.6	9.7	
		843	2.4	15.7	24.5	
		843	1.8	16.91	28	
		843	2.4	12.6	22.9	

$(k_{obs}D)/\bar{v}^2$ is a correction for axial diffusion, and $(k_{obs}r^2)/48D$ is a correction for radial diffusion. The diffusion coefficient, D, for I_2 in He was calculated to be 256 cm^2 s^{-1} Torr^{-1}, using the standard equation[28] and twice the diffusion volume of xenon as an approximation to that for I_2. The maximum correction to k_1' for effects of diffusion was found to be 2%.

The weighted-average temperature-independent rate coefficient for the reaction is $k_1 = (1.5 \pm 0.5) \times 10^{-12}$ cm^3 molecule^{-1} s^{-1}.

3.1.2. Further Evidence for a Reaction between NO_3 and I_2. As the measurements reported here represent the first indications of a reaction between the iodine molecule and the nitrate radical, it is desirable to characterize the reaction system further than a simple determination of the kinetics of the disappearance of I_2 in the presence of NO_3. One alternative explanation of the results might be that I_2 reacts with a species that is present in the flow reactor at concentrations proportional to $[NO_3]$. Unfortunately, we were unable to carry out experiments in which $[I_2] \gg [NO_3]$ and follow the decay of $[NO_3]$ because a deposit, which had a strong absorption at $\lambda = 662$ nm, formed on the windows of the White cell when $[I_2] \simeq [NO_3]$, even at the lowest $[NO_3]$ usefully measurable with the dual-beam spectrometer arrangement.

We were particularly concerned that reaction with fluorine atoms or FO radicals was the cause of the reduction in $[I_2]$. Atomic fluorine is known to react rapidly with molecular iodine

$$F + I_2 \rightarrow IF + I \quad (6)$$

$$k_6 = 4 \times 10^{-10} \text{ cm}^3 \text{ molecule}^{-1} \text{ s}^{-1}$$ [29]

and F atoms are present in the flow reactor because they are used in the generation of the NO_3 radical. FO radicals are formed in a secondary reaction between F and NO_3

$$F + NO_3 \rightarrow FO + NO_2 \quad (7)$$

$$k_7 = 3 \times 10^{-11} \text{ cm}^3 \text{ molecule}^{-1} \text{ s}^{-1}$$ [13]

F atoms can then be regenerated by the subsequent self-reaction of FO

$$FO + FO \rightarrow 2F + O_2 \quad (8)$$

$$k_8 = 1.5 \times 10^{-11} \text{ cm}^3 \text{ molecule}^{-1} \text{ s}^{-1}$$ [30]

Although the concentrations of F and FO should be very small compared with $[NO_3]$, as we always had a large excess of nitric

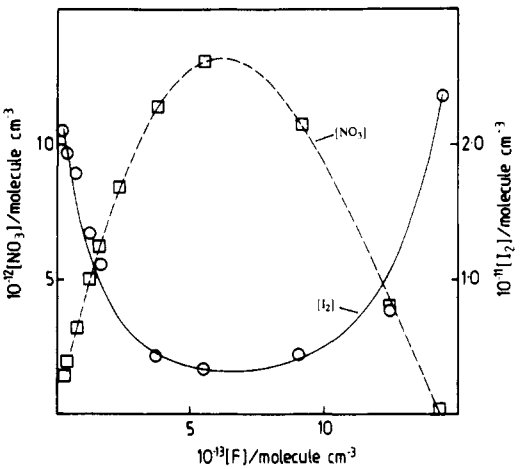

Figure 4. Simulated and experimental concentration profiles of I_2 and NO_3 as a function of $[F]_0$. $T = 297$ K, $P_{ft} = 1.8$ Torr, reaction contact time to center of fluorescence cell block (for detection of I_2) = 89 ms and to White cell (for detection of NO_3) = 111 ms.

(28) Perry, R. H.; Chilton, C. H. *Chemical Engineers Handbook*; McGraw-Hill, Kogakusha, Ltd.: Tokyo, 1973.
(29) Appelman, E. H.; Clyne, M. A. A. *J. Chem. Soc., Faraday Trans. 1* **1975**, *71*, 2072.
(30) NASA Panel for Data Evaluation. *Chemical Kinetics and Photochemical Data for Use in Stratospheric Modeling, No. 9*; JPL Publication 90-1; Jet Propulsion Laboratory: Pasadena, CA, 1990.

TABLE II: Experimental Data for the Reaction $I_2 + NO_3$ at Elevated Temperatures

T, K	P_{ft}, Torr	$\bar{v}$, cm s^{-1}	$10^{-11}[I_2]$, molecules cm^{-3}	$10^{-12}[NO_3]$, molecules cm^{-1}	k_1', s^{-1}	$10^{12}k_1$, cm^3 molecule^{-1} s^{-1}
336	1.3	1274	3.4	5.7	10.9	
		1274	3.4	2.9	4.7	
		1322	5.9	7.5	21.4	
		1322	5.0	3.6	7.4	
		1322	4.3	2.5	6.3	
		1322	4.0	3.6	8.8	1.6 ± 0.1
	1.5	1227	2.6	11.3	22.3	
		1233	2.4	8.1	24.1	
		1235	3.0	10.9	24.8	
	1.3	1239	9.0	12.5	27.55	
		1251	9.0	13.9	24.0	
		1241	10.0	9.7	15.0	
353	1.2	1361	7.0	17.3	26.0	
		1355	10.0	22.2	35.1	
		1368	6.6	8.6	14.0	1.6 ± 0.1
		1358	10.0	22.6	34.7	
		1420	7.7	17.1	27.6	
377	1.2	1489	3.5	12.1	17.6	
		1600	6.0	15.5	26.3	
		1576	3.0	11.2	18.8	
		1600	3.0	8.2	13.3	
		1579	4.0	19.0	29.6	1.6 ± 0.1
		1600	7.0	15.0	24.6	
		1579	9.0	10.3	15.3	
	1.3	1400	3.0	5.5	9.4	
		1399	3.5	11.3	19.2	
		1408	4.0	14.0	22.6	
393	1.2	1580	5.1	13.7	22.5	
		1609	3.0	17.2	28.9	
		1594	4.0	6.0	11.8	
		1508	4.7	8.6	14.5	1.7 ± 0.1
		1588	4.3	13.1	22.2	
		1571	9.0	17.1	29.8	
		1596	4.0	16.7	31.3	
		1588	10.0	27.5	44.7	
427	1.3	1569	3.0	12.6	23.6	
		1596	4.0	9.7	19.2	
		1571	4.0	7.0	11.1	
		1591	7.0	11.0	20.3	1.6 ± 0.2
		1579	7.0	14.0	19.0	
		1571	10.0	21.4	35.2	
		1591	3.1	18.6	26.8	
		1572	5.3	13.3	19.5	

acid compared to atomic fluorine in the system, we still thought it desirable to investigate the possible loss of I_2 in reaction 6. We performed an experiment in which the concentrations of I_2 and NO_3 were monitored simultaneously, at a fixed contact time, as the initial concentration of fluorine atoms was varied. The results are shown in Figure 4. The profile of the NO_3 concentration is as expected, $[NO_3]$ increasing with [F] to a maximum value and then decreasing as it is consumed by reaction with F and FO. The profile of the iodine concentration, however, is anticorrelated with that of $[NO_3]$. [F], and therefore [FO], appears to have no influence on $[I_2]$ until all of the NO_3 has disappeared, and then there is an abrupt loss in $[I_2]$ (not shown in the figure). The iodine profile thus suggests that [F] in the reactor is low until all of the NO_3 has been consumed and, further, that when HNO_3 is in excess over F, the loss in $[I_2]$ is due solely to reaction with NO_3.

The smooth curves in Figure 4 are the results of a model simulation of the experimental data (the boxes and circles in the diagram); a numerical integration package (FACSIMILE[31,32]) was used. The model simulation utilized the reaction scheme shown in Table III. The calculations were performed for a series of different starting conditions of $[F]_0$ and $[HNO_3]_0$. Neither of these quantities is measured directly in our experiments, but they can be fixed by comparison of the predicted $[NO_3]$ with the measured concentrations. The maximum concentration of the nitrate radical, $[NO_3]_{max}$, is a function of both $[F]_0$ and $[HNO_3]_0$,

TABLE III: Reaction Scheme for the System F + HNO_3 and I_2[a]

reaction	rate constant, cm^3 molecule^{-1} s^{-1}	ref
$F + HNO_3 \rightarrow HF + NO_3$	2.3×10^{-11}	1
$F + NO_3 \rightarrow FO + NO_2$	3.0×10^{-11}	1
$FO + FO \rightarrow F + F + O_2$	1.5×10^{-11}	30
$FO + NO_3 \rightarrow FO_2 + NO_2$	1.0×10^{-12}	1
$NO_3 + NO_3 \rightarrow NO_2 + NO_2 + O_2$	2.3×10^{-16}	1
$NO_3 \rightarrow$ products	0.1[b]	this work
$NO_2 + NO_3 \xrightarrow{M} N_2O_5$	7.2×10^{-14}	1
$N_2O_5 \xrightarrow{M} NO_2 + NO_3$	8.3×10^{-3} [b]	1
$F + O_2 \xrightarrow{M} FO_2$	2.9×10^{-16}	30
$NO_2 + NO_3 \rightarrow NO + NO_2 + O_2$	8.26×10^{-16}	1
$NO + NO_3 \rightarrow NO_2 + NO_2$	3.0×10^{-11}	1
$F + NO_2 \rightarrow FO + NO$	6.7×10^{-14}	30
$FO + NO_2 \xrightarrow{M} FONO_2$	2.4×10^{-14}	30
$FO + NO \rightarrow F + NO_2$	2.6×10^{-11}	30
$I_2 + NO_3 \rightarrow I + IONO_2$	1.5×10^{-12}	this work
$I_2 + F \rightarrow IF + I$	4.0×10^{-10}	29

[a] [M] = 6.5×10^{16} molecules cm^{-3}. [b] Units are s^{-1}.

but for a given $[HNO_3]_0$ it has a unique value as $[F]_0$ is varied. Our procedure was thus to match the experimental and calculated values of $[NO_3]_{max}$ by using a range of $[F]_0$. The value of $[F]_0$ used in the simulations to obtain this maximum serves to define the absolute $[F]_0$ at this point on the $[NO_3]$ curve. Other positions on the abscissa of Figure 4 can then be determined from the values of $[F]_0$ needed to match the calculated and experimentally measured NO_3 concentrations. Since each individual experimental

(31) Curtis, A. R. Technical Report AERE-R 9352, Harwell, 1979.
(32) Pilling, M., Smith, I. W. M., Eds. *Modern Gas Kinetics Theory, Experiment and Application*; Blackwell Scientific Publications: Oxford, 1987.

TABLE IV: Experimental Data for the Reaction I + NO_3, Using a Microwave Discharge through I_2 as a Source for I

T, K	P_{ft}, Torr	$\bar{v}$, cm s^{-1}	10^{-11}[I], molecules cm^{-3}	10^{-12}[NO_3], molecules cm^{-3}	k_2', s^{-1}	$k_2'_{corr}$, s^{-1}	f
294	1.8	1076	0.7	3.4	1080	1352	1.25
	1.7	1137	0.6	2.4	845	1002	1.19
	1.7	1123	0.5	1.2	476	526	1.11
295.5	1.7	1135	0.3	2.0	802	946	1.18
	1.7	1135	0.4	1.0	397	432	1.09
	1.7	1135	0.4	4.0	1491	1981	1.33
	1.7	1134	1.5	2.4	1017	1245	1.22
294	1.7	1158	0.7	2.1	886	1058	1.19
	1.7	1153	0.8	2.1	818	965	1.18
	1.7	1195	0.7	2.1	891	1063	1.19
295.5	1.0	1071	1.0	0.7	458	497	1.08

TABLE V: Experimental Data for the Reaction I + NO_3, Using I_2 + O as a Source of I

T, K	P_{ft}, Torr	$\bar{v}$, cm s^{-1}	10^{-11}[I], molecules cm^{-3}	10^{-12}[NO_3], molecules cm^{-3}	k_2', s^{-1}	$k_2'_{corr}$, s^{-1}	f
298	2.1	1342	0.4	1.6	579	661	1.14
	2.1	1342	0.4	1.9	852	1030	1.21
299.5	2.1	1348	0.5	0.9	366	399	1.09
	2.1	1330	0.5	2.4	857	1037	1.21
298	1.9	1429	0.3	1.0	557	626	1.12
	1.9	1427	0.1	1.0	543	609	1.12
	1.9	1429	0.3	1.9	841	999	1.19
	1.9	1421	0.4	3.1	1302	1681	1.29
299	1.9	1424	0.2	2.0	1023	1257	1.23
	1.9	1424	0.5	0.6	345	372	1.08

[NO_3] corresponds to a measured [I_2], the [F]$_0$ scale is also fixed for the I_2 determinations. The coincidence of the simulated and observed profiles of [I_2] is, we feel, conclusive evidence that the loss in [I_2] is indeed due to a reaction with the nitrate radical. Note, however, that in the case of the NO_3 concentrations the agreement between experimental and simulated values is as close as it is only because the two sets of data were forced to match.

One pathway for the reaction, which we shall show in the Discussion section is the most probable one, is the formation of iodine atoms and iodine nitrate

$$I_2 + NO_3 \rightarrow I + IONO_2 \qquad (1a)$$

It was possible to monitor [I], simultaneously with I_2 and NO_3, as explained in section 2. However, no fluorescence from I atoms was observed (see section 4.1.3).

3.2. Reaction between NO_3 and I. *3.2.1. Generation of I. 3.2.1.1. Formation of I Atoms by Use of a Microwave Discharge on I_2/He.* For concentrations of I_2 larger than about 2×10^{11} molecules cm^{-3}, a microwave discharge passed through the flow of I_2 in He resulted in an intense chemiluminescent emission in the wavelength region 170–200 nm. This emission was independent of the exciting radiation from the atomic light source and did not occur for a discharge through a flow of He only. The signal increased with increasing loss of molecular iodine in the discharge. There was a period at the beginning of each day of experiments during which no resonance fluorescence from I atoms was seen, after which the fluorescence would appear. We interpret this initial period as the time required to passivate the walls of the flow reactor so that I was not rapidly lost. We attempted to inject I atoms along the movable injector, but we always saw an emission, independent of the exciting atomic radiation, even for concentrations of I_2 lower than 2×10^{11} molecules cm^{-3}. We were therefore restricted to experiments for which NO_3 radicals were formed in the sliding injector and I atoms in the main flow tube, and even then we could only use concentrations of iodine lower than 2×10^{11} molecules cm^{-3}.

3.2.1.2. Formation of I Atoms by the Reaction between I_2 and O. The fast interaction between O atoms and iodine molecules (reaction 4) was used as an alternative source of I, in order to validate the experimental observations found with the discharge acting directly on I_2 and because of the difficulties associated with that method for generation of I. In the few previous kinetic investigations involving I atoms, an indirect method for their production has been the favored approach.[33,34] When I atoms were generated in the main body of the flow reactor using relatively low [O], we found that the fluorescence signal changed, in the absence of NO_3, on altering the position of the movable injector, in the sense that the signal decreased as the distance between the injector tip and the observation zone increased. This effect was not observed when the direct source of I was used. For our experimental conditions, in which approximately 25% of the carrier gas is admitted via the sliding injector, we find that movement of the injector tip by 10 cm upstream from the center of the observation region results in a small change ($\simeq$+0.4%) in the time elapsed between generation and observation for a species, for example I or IO, in the main body of the flow reactor. The corresponding change in the overall surface-to-volume ratio (S:V) experienced by the species is much larger at about −10%. Thus the [I] decreases as the S:V decreases, indicating that iodine atoms must be *created* at the surface of the flow reactor.

When the concentration of O atoms used was large compared with [I_2], the influence of injector position was suppressed. However, when investigating the reaction between I and NO_3, we could not work under conditions in which [O] > 2[I_2], because excess oxygen atoms then react rapidly with the nitrate radical

$$O + NO_3 \rightarrow NO_2 + O_2 \qquad (9)$$

$$k_9 = (1.7 \pm 0.6) \times 10^{-11} \text{ cm}^3 \text{ molecule}^{-1} \text{ s}^{-1}$$ [35]

and complicate or invalidate the analysis of the experimental data.

3.2.2. Kinetics of the Reaction of NO_3 with I. The study of the kinetics of the reaction between I and NO_3 necessitates the simultaneous in-situ production of two "open-shell" reactants. Thus, because precursor molecules, and byproducts, from the synthesis of the reactant compounds are inevitably present in the flow reactor, the operating conditions for the study of this particular reaction system had to be carefully controlled.

The nitric acid used in the formation of nitrate radicals has a large absorption cross section in the region of the I atom emission [$\sigma(\lambda$=190 nm) = 1.56×10^{-17} cm^2 $molecule^{-1}$ [30]], so that to minimize the reduction in fluorescence signal from the iodine atoms, only a small excess of HNO_3 over F was employed.

(33) Clyne, M. A. A.; Cruse, H. W. *J. Chem. Soc., Faraday Trans. 2* **1972**, *68*, 1377.
(34) Jenkin, M. E.; Cox, R. A.; Mellouki, A.; LeBras, G.; Poulet, G. *J. Phys. Chem.* **1990**, *94*, 2927.
(35) Canosa-Mas, C. E.; Carpenter, P. J.; Wayne, R. P. *J. Chem. Soc., Faraday Trans. 2* **1989**, *85*, 697.

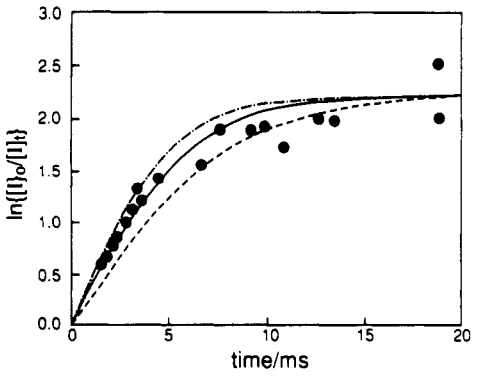

Figure 5. Pseudo-first-order plot for I + NO_3 (I_2 + O as source of I). T = 299 K, P_{ft} = 1.9 Torr, $[I_2]_0 = 5 \times 10^{10}$ molecules cm^{-3}, $[NO_3]_0 = 6 \times 10^{11}$ molecules cm^{-3}. The curves are the results of a simulation of the experimental data as described in section 4.2.2: (---) $k_2 = 4.7 \times 10^{-10}$ cm^3 molecule^{-1} s^{-1}, $k_{18} = 35$ s^{-1}; (—) $k_2 = 6.1 \times 10^{-10}$ cm^3 molecule^{-1} s^{-1}, $k_{18} = 45$ s^{-1}; (-·-) $k_2 = 7.4 \times 10^{-10}$ cm^3 molecule^{-1} s^{-1}, $k_{18} = 55$ s^{-1}.

We studied the kinetics of the reaction between I and NO_3 at ambient temperature only and at a pressure of about 2 Torr. The experimental details for each measurement of the decay in [I] at different NO_3 concentrations are given in Tables IV and V for the two sources of I atoms. We used pseudo-first-order conditions with NO_3 in excess. The concentrations of I atoms listed in the tables are upper limits based on the estimate of the sensitivity discussed earlier.

We observed that some of the pseudo-first-order plots exhibited pronounced curvature at contact times longer than 3 ms, irrespective of the means of generation of I atoms. Figure 5 illustrates this phenomenon, the experimental conditions being stated in the figure caption. The results are indicative of the establishment of a steady-state concentration of I atoms in the chemical system. A closer inspection of the data revealed that, with the direct source of I, linear plots were obtained for experiments performed at the beginning of each day, strongly suggesting that the regeneration of I atoms at longer contact times for subsequent experiments originates in reactions at the walls of the flow tube. All pseudo-first-order plots for which I_2 + O was used as a source of I atoms showed a curvature indicative of a steady state of I at longer contact times.

We assumed that the initial, linear, portion of the graphs represented the loss of I from reaction with NO_3 radicals. The initial slope was thus taken to represent k_2', the pseudo-first-order rate coefficient. The large values of k_2' found for this reaction mean that a correction to the observed k_2' for axial and radial diffusion is necessary. The diffusion coefficient for I in He was calculated to be 360 cm^2 s^{-1} Torr^{-1}, using the same procedure as described earlier for I_2. The correction factors, f, for the initial slopes of the pseudo-first-order plots, k_2', were calculated using eq i. Values of k_2', $k_{2\,corr}'$ ($=fk_2'$), and f are given in Tables IV and V. The maximum correction for diffusion is 33% (Table IV). Values of $k_{2\,corr}'$ are used, along with the corresponding $[NO_3]$, to give the second-order plot shown in Figure 6. The data in Figure 6 suggest that the initial loss in [I] is independent of the mode of its generation. The gradient of the plot indicates that the reaction studied is extremely rapid, giving $k_2 = (4.5 \pm 0.7) \times 10^{-10}$ cm^3 molecule^{-1} s^{-1}. The intercept in Figure 6 is 90 ± 144 s^{-1}. The errors quoted are the 95% confidence limits limits of a linear least-squares fit to the data points. The overall accuracy is estimated to be ±42% (26% error in the estimation of $[NO_3]$ and 15% error from the 95% confidence limits) so that $k_2 = (4.5 \pm 1.9) \times 10^{-10}$ cm^3 molecule^{-1} s^{-1}. The curvature in the pseudo-first-order plots, the magnitude of the rate coefficient, and the intercept in Figure 6 will be discussed in section 4.2.

4. Discussion

Neither of the reactions NO_3 + I_2 or NO_3 + I has been studied or, apparently, even observed, before, partly because the chemistry of the nitrate radical has only recently been the subject of intensive investigation[1] and partly, in the instance of the reaction with I,

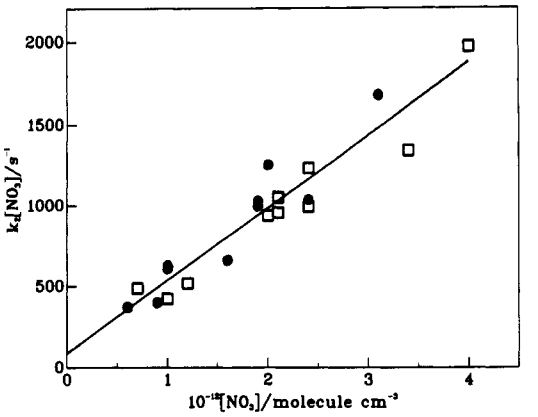

Figure 6. Second-order plot for the reaction I + NO_3: (□) I_2 + microwave discharge; (○) I_2 + O as sources for I atoms.

because the reaction is popularly assumed to be endothermic and therefore unlikely to occur in the gas phase. We therefore begin the discussion of the data presented in the previous section with an analysis of potential alternative explanations for the observed changes in $[I_2]$ and [I] in the presence of NO_3. The probable mechanisms of the interactions of NO_3 with the iodine species are then considered. Finally, we speculate about the ramifications of the magnitudes of the thermal rate coefficients measured in this work with regard to the tropospheric chemistry of iodine, NO_3 and ozone.

4.1. Reaction between NO_3 and I_2. *4.1.1. Interfering Chemical Losses of I_2.* We have already shown that the loss in $[I_2]$ cannot be attributed to the rapid reaction

$$I_2 + F \rightarrow IF + I \qquad (6)$$

Furthermore, we observed no loss in $[I_2]$ on addition of F_2 and HNO_3 to the flow reactor without any discharges excited.

The action of a microwave discharge on fluorine flowing through Pyrex tubing is known to produce oxygen atoms,[36] possibly by the reaction of F with SiO_2, the ratio of [O] to [F] being about 0.1. We do not expect the O atoms to contribute to the decay in $[I_2]$ through reaction 4 since O will react preferentially with NO_3 (reaction 9), which is present in high concentrations compared with I_2. In addition, there is a reaction time of about 35 ms within the sliding injector before the NO_3 radicals and any O atoms formed by the action of F at the walls are admitted to the main flow.

4.1.2. Potential Contributions to the Observed Emission Signal at λ = 539 nm. F_2 is known to react with I_2[37]

$$F_2 + I_2 \rightarrow I_2F + F \qquad (10)$$

Although the rate coefficient has not been measured, it is expected to be small and, as noted in the previous section, $[I_2]$ did not change on addition of F_2 to the flow reactor. Birks and co-workers[38] observed chemiluminescence from electronically excited IF molecules in the wavelength range 450–750 nm on mixing I_2 and F_2, and Kahler and Lee[37] have assigned the emission to the production of IF* by the secondary reaction between F atoms and I_2F

$$I_2F + F \rightarrow IF^* + IF \qquad (11)$$

Although the initial reaction, (10), is slow, the subsequent step, (11), is expected to be rapid and chemiluminescence from IF* could supplement the observed LIF signal from I_2. However, no chemiluminescence was observed in the absence of laser excitation at λ = 514.9 nm for typical experimental conditions.

The emission signal was also checked for contributions from IF* for those experiments in which [F] was sufficiently high to

(36) Clyne, M. A. A.; McKenny, D. J.; Walker, R. F. *Can. J. Chem.* **1973**, *51*, 3596.
(37) Kahler, C. C.; Lee, Y. T. *J. Chem. Phys.* **1980**, *73*, 5123.
(38) Birks, J. W.; Gabelnick, S. D.; Johnston, H. S. *J. Mol. Spectrosc.* **1975**, *57*, 23.

deplete $[NO_3]$. As shown in Figure 4, there are in general two possible values of $[F]_0$, and, correspondingly, two emission signals, of equal intensity, at $\lambda = 539$ nm at a fixed $[HNO_3]_0$. A scan of the wavelength dependence of this emission for each of the two values of $[F]_0$ showed that the spectra of the emissions were identical. Thus, the increase in emission signal with lower $[NO_3]$ but higher $[F]_0$ could be unambiguously assigned to an increase in $[I_2]$. We therefore conclude that the time-dependent loss in $[I_2]$ in the presence of NO_3 is in reality due to reaction 1.

4.1.3. Mechanism of the Reaction between NO_3 and I_2. Several pathways can be postulated for reaction between I_2 and NO_3

$$I_2 + NO_3 \rightarrow I + IONO_2 \quad \text{see text} \qquad (1a)$$

$$\rightarrow I + IO + NO_2 \quad \Delta H_r = 120.2 \text{ kJ mol}^{-1} \qquad (1b)$$

$$\rightarrow I + O_2 + INO \quad \Delta H_r = 101.3 \text{ kJ mol}^{-1} \qquad (1c)$$

$$\rightarrow IO + INO_2 \quad \Delta H_r = 40.4 \text{ kJ mol}^{-1} \qquad (1d)$$

The heats of formation of all species except $IONO_2$ and IO, are given by Atkinson et al.[39] The heat of formation of IO, $\Delta H_f(IO) = 107$ kJ mol^{-1}, is taken from Reddy et al.[40] and is 65 kJ mol^{-1} less than currently recommended in most evaluations; that for NO_3 is assumed to be 64.4 kJ mol^{-1},[1] and there appears to be no published value for ΔH_f of $IONO_2$. Routes 1b–d are endothermic and are unlikely to occur at ambient temperatures. Route 1a thus seems to us to be the most likely reaction pathway; we shall discuss the heat of formation of $IONO_2$ in section 4.1.6. NO_3 is presumably unreactive toward the other diatomic halogen molecules, F_2, Cl_2, and Br_2, because of the endothermicity of the bimolecular processes

$$F_2 + NO_3 \rightarrow F + FONO_2 \quad \Delta H_r = 25 \pm 3 \text{ kJ mol}^{-1} \qquad (12)$$

$$Cl_2 + NO_3 \rightarrow Cl + ClONO_2 \quad \Delta H_r = 83.3 \text{ kJ mol}^{-1} \qquad (13)$$

$$Br_2 + NO_3 \rightarrow Br + BrONO_2 \quad \Delta H_r = 37 \pm 23 \text{ kJ mol}^{-1} \qquad (14)$$

In fact, one of the reverse reactions, $Cl + ClONO_2$ ($k_{-13} = 1.2 \times 10^{-11}$ cm^3 molecule^{-1} s^{-1}),[41] has been used as a source of NO_3 radicals in laboratory studies.[1,12] Even if the reaction between I_2 and NO_3 gives iodine atoms as a product for a typical concentration of I_2 of 2×10^{11} molecules cm^{-3}, reaction 1a followed by reaction 2 leads to a steady-state [I] of $\{(k_{1a}/k_2)[I_2]\} = 10^9$ molecules cm^{-3}, which is equivalent to the detection limit of our atomic resonance fluorescence system. Thus, we do not necessarily expect to observe fluorescence from I formed in reaction 1a. Further understanding of the pathway for the reaction can be gained by consideration of other reactions of I_2 with radical species X. The formation of a deposit under certain experimental conditions in the I_2 and NO_3 system offers circumstantial evidence for the occurrence of reaction 1a as will be shown below.

4.1.4. A Comparison with Other Measurements of Reactions between I_2 and X. Several reactions of radical species with molecular iodine have been studied in the gas phase.[26,29,42,43] In general, the reactivity of radical species toward halogen molecules[44] increases with increasing electron affinity of the radical and decreases with increasing ionization potential of the molecule. The results of a classical trajectory study[45] of the reaction $O(^3P) + I_2 \rightarrow OI + I$ show that the transition from reactants to products proceeds via a long-lived complex consisting of a near-linear, asymmetrical, configuration. Kosmas and Williams[45] choose that potential energy surface for the reaction which is in best agreement with the results of a crossed molecular beam study of the reaction by Grice,[46] and a calculation of the thermal rate constant from the trajectory studies yields $k_4 = 9.08 \times 10^{-11}$ cm^3 molecule^{-1} s^{-1}, which is close to the measured value of Ray and Watson.[26] We can envisage a similar potential energy surface for the $I_2 + NO_3$ reaction; a reactive trajectory would therefore involve the formation of a long-lived collision complex, $(I_2NO_3)^\dagger$, which falls apart to give I and $IONO_2$. The increase in the complexity of NO_3 with respect to O leads to a smaller A factor for the rate coefficient.[47] The observed lack of activation energy for reaction 1 coincides with the assumption that the reaction proceeds via a long-lived intermediate complex.[47]

4.1.5. Deposition of Iodine-Containing Species: Evidence for Route 1a? Deposits of substances likely to contain iodine were observed explicitly in two chemical systems. First, when operating with large concentrations of I_2 and O atoms, we observed the buildup of a deposit which absorbed radiation in the wavelength region 180–200 nm. The deposit disappeared on leaving it exposed to the air overnight. Second, deposits in the flow reactor were observed when iodine molecules and nitrate radicals were present in similar concentrations. In this instance, the deposit absorbed radiation at $\lambda = 662$ nm, although a spectrum of the transmission of a contaminated window from the White cell over the wavelength range 400–700 nm failed to show any features. We shall consider first the $I_2 + O$ reaction system as it is simpler than the $I_2 + NO_3$ system.

The reaction between O and I_2 produces IO radicals as well as I atoms. Addition of NO to the system should result in an increase in [I] as IO reacts rapidly with NO

$$IO + NO \rightarrow I + NO_2 \qquad (15)$$

$$k_{15} = (2.8 \pm 0.2) \times 10^{-11} \text{ cm}^3 \text{ molecule}^{-1} \text{ s}^{-1}$$ [48]

However, changes in the signal from I atom resonance fluorescence were small on addition of NO, and we found that NO also fluoresced in the detection region on excitation by the iodine atomic lines emitted by the lamp. It is possible that the atomic emission at $\lambda = 184.45$ nm[49] is causing electronic excitation of NO as Hikida et al.[50] have observed a weak fluorescence when NO is illuminated by light of $\lambda = 184.9$ nm. Other workers[42,51] have successfully determined [IO] in a low-pressure discharge-flow system by monitoring the increase in [I] on addition of NO. The small changes in [I] on addition of NO to our system are therefore indicative of low concentrations of IO in the flow reactor. It thus seems likely that the rate of loss of IO on the walls of the flow tube is large.

The IO radical is known to be reactive toward surfaces.[52,53] Clyne and Cruse[53] found that a deposit formed in a low-pressure discharge-flow system containing I and O_3 and that loss of IO was more rapid on the deposit than on the clean surface of the flow cell. Cox and Coker[54] have reported the formation of an aerosol, thought to be I_4O_9, in a gas-phase system containing I and O_3. The aerosol exhibited a large absorption cross section at $\lambda = 200$ nm. It therefore seems reasonable to us to assume that the deposit formed in our flow system when I, IO, I_2, and O_2 are present is an oxide of iodine, I_xO_y.

The reaction between I and NO_3 is likely to produce IO radicals so that reaction 1a followed by reaction 2 results in the formation of IO and therefore in the formation of the deposit I_xO_y. That no deposit was observed in the chemical system used to study the

(39) Atkinson, R.; Baulch, D. L.; Cox, R. A.; Hampson, Jr., R. F.; Kerr, J. A.; Troe, J. *J. Phys. Chem. Ref. Data* **1989**, *18*, 881.
(40) Reddy, R. R.; Rao, T. U. R.; Reddy, A. S. R. *Indian J. Pure Appl. Phys.* **1989**, *27*, 243.
(41) Kurylo, M. J.; Knable, G. L.; Murphy, J. L. *Chem. Phys. Lett.* **1983**, *101*, 73.
(42) Loewenstein, L. M.; Anderson, J. G. *J. Phys. Chem.* **1985**, *89*, 5371.
(43) Phillips, L. *Can. J. Chem.* **1965**, *51*, 3596.
(44) Loewenstein, L. M.; Anderson, J. G. *J. Phys. Chem.* **1987**, *91*, 2993.
(45) Kosmas, A. M.; Williams, R. J. *Chem. Phys.* **1990**, *140*, 413.
(46) Grice, R. *Acc. Chem. Res.* **1981**, *14*, 37.
(47) Smith, I. W. M. *Kinetics and Dynamics of Elementary Gas Reactions*; Butterworth: London, 1980.
(48) Inoue, G.; Suzuki, M.; Washida, N. *J. Phys. Chem.* **1983**, *79*, 4730.
(49) Kiess, C. C.; Corliss, C. H. *J. Res. Natl. Bur. Stand., Sect. A* **1959**, *63*, 1.
(50) Hikida, T.; Washida, N.; Nakajima, S.; Yagi, S.; Ichimura, T.; Mori, Y. *J. Chem. Phys.* **1975**, *63*, 5470.
(51) Maguin, F.; Mellouki, A.; Laverdet, G.; Poulet, G.; LeBras, G. *Int. J. Chem. Kinet.* **1991**, *23*, 237.
(52) Martin, D.; Jourdain, L.; Laverdet, G.; LeBras, G. *Int. J. Chem. Kinet.* **1987**, *19*, 503.
(53) Clyne, M. A. A.; Cruse, H. W. *Trans. Faraday Soc.* **1970**, *66*, 2227.
(54) Cox, R. A.; Coker, G. B. Technical Report AERE-R 10581, Harwell, 1982.

reaction between I and NO_3 is probably a consequence of concentrations of I_2 and NO_3 that were more than an order of magnitude smaller than those used in the study of the reaction between I_2 and NO_3.

Other possibilities for the composition of the deposit include $IONO_2$ or $(IF)_x$. Appelman and Clyne[29] found that the species IF polymerizes rapidly on the uncoated glass walls of a low-pressure flow reactor

$$IF + \text{wall} \rightarrow (IF)_x(s) \qquad (16)$$

$$k_{16} = 200\text{–}500\ s^{-1}$$

The molecule IF may be formed in the flow tube by the reaction between F and I_2. It was noted at the beginning of this section that a spectrum of the deposit formed on the White cell windows failed to show any features over the wavelength range $400 < \lambda < 700$ nm. It is now apparent that further investigation of the absorption characteristics of the deposit, formed during the course of the reaction between I_2 and NO_3, at wavelengths around 200 nm is worthwhile in order to resolve whether the solid is the same as that observed in the $O + I_2$ reaction system.

4.1.6. Estimation of the Heat of Formation of $IONO_2$. If we assume that the reaction between I_2 and NO_3 occurs entirely by route 1a, then the large rate constants measured for the reaction must mean that the process is exothermic or thermoneutral. Thus, $\Delta H_f(IONO_2) + \Delta H_f(I) - \Delta H_f(I_2) - \Delta H_f(NO_3) \leq 0$, and substitution of values for the heats of formation of all species other than $IONO_2$ gives an upper limit for the heat of formation of iodine nitrate of $\Delta H_f(IONO_2) \leq 21 \pm 3$ kJ mol^{-1}.

4.2. Reaction of I with NO_3. Since the rate coefficient for the reaction

$$I + NO_3 \rightarrow IO + NO_2 \qquad (2)$$

was derived from the initial (constant) slope of the pseudo-first-order plots of the experimental data, we must consider factors which might interfere with that part of the measurements. Possible contributions to the observed loss in [I] on addition of NO_3 to the flow reactor include homogeneous reaction of I with species other than NO_3 and heterogeneous reactions of I, IO, or NO_3.

4.2.1. Possible Homogeneous Reactions of I with Species Other Than NO_3. The complex nature of the reaction conditions means that there are a number of reactive species in the flow system during the course of the interaction of I with NO_3. However, any radical products of secondary reactions in the synthesis of NO_3, for example FO, are present in lower concentration than that of NO_3, and therefore any transformation involving these species would have to exhibit a *larger* second-order rate coefficient than that derived for the reaction with NO_3. We shall show that the value for k_2 measured in this work is already 60% of the hard-sphere collision frequency factor for I and NO_3 (section 4.2.3), and thus reaction with other radical species present in lower concentration than NO_3 is unlikely to influence the initial decay in [I].

Iodine atoms are known[55] to react with I_2, NO_2, and NO, all of which are present in our system. The overall effect of the reactions is the recombination of iodine atoms via the atom–molecule complex mechanism.[56] The rate-determining step is the addition of I to M, and the measured rate coefficients[55,57] for M = NO, NO_2, and I_2 are all too small for the reactions to be significant at the concentrations of NO, NO_2, or I_2 present in our system.

Next we turn to species present in concentrations greater than that of NO_3. We used low concentrations of HNO_3 in order to minimize the reduction in signal due to optical absorption at $\lambda = 170\text{–}200$ nm by HNO_3. It can readily be shown that a significant influence of the change in $[HNO_3]_0$ on addition of F to the flow reactor on the I atom signal would be manifest as an intercept, $\sigma[HNO_3]l$, in the pseudo-first-order plot. As all pseudo-first-order graphs have zero intercepts, we can assume that the absorption of radiation from I by HNO_3 has a negligible effect on the kinetic analysis employed in this work. The intensity of atomic fluorescence did not vary with the addition of F_2 to the flow apparatus. The rate coefficient for the reaction of I with F_2

$$I + F_2 \rightarrow IF + F \qquad (17)$$

$$k_{17} = (1.9 \pm 0.4) \times 10^{-14}\ \text{cm}^3\ \text{molecule}^{-1}\ \text{s}^{-1}$$ [58]

is 4 orders of magnitude less than that observed for $I + NO_3$ and is too low to have an impact on [I] in our system.

4.2.2. Possible Heterogeneous Reactions of I. Several experimental observations reported in section 3 suggest that rapid heterogeneous processes occur in the flow reactor, and their nature will be considered later. Of more immediate concern is the quantitative influence of reactions at the surface of the flow reactor on the observed time-dependent loss of [I]. Three different transformations require critical appraisal: they are (a) heterogeneous loss of I in the presence of NO_3, (b) suppression by NO_3 of processes which produce I at the surface, and (c) heterogeneous *generation* of I in the presence of NO_3. Processes a and b could result in an overestimate of the rate constant for the homogeneous reaction between I and NO_3, whereas process c might lead to an underestimate of it.

Two possible scenarios can be considered[59] for a change in the rate of wall loss, k_w, of I on addition of NO_3 to the flow reactor: (i) a "step" in the value of k_w, which would be manifest as an intercept in the second-order plot, and (ii) an alteration in k_w that is proportional to the concentration of the reactant added. In case ii the intercept in the second-order plot should remain zero, and the change in k_w becomes incorporated into the slope of the graph. The intercept in Figure 6 is not distinguishable from zero; in any case, a step change in the surface efficiency, γ, should not introduce errors into the calculation of the rate coefficient. The second scenario is potentially more troublesome. However, using Walker's method[60] to solve the continuity equations shows that even if γ increases up to unity (a very unlikely situation), the correction to the observed value of k_2 would be less than 15%.

I atoms can be regenerated at the surface of the flow reactor by either IO or some other reactive species, Y, in the $I_2 + O$ reaction system. The addition of NO_3 to the system may suppress these regeneration processes and could therefore contribute to the observed loss in [I] in an indirect manner. However, the loss in [I] consistent with removal of Y from the system by NO_3 is estimated (by assuming that the surface in contact with NO_3 no longer produces I) to be 10–35 times lower than that observed on addition of NO_3 to the flow tube. Thus, suppression of processes which generate I at the surface can have only a negligible influence on the concentration–time profile of I.

Some of the pseudo-first-order plots for the reaction between I and NO_3 exhibited pronounced curvature irrespective of the means of generation of I atoms (Figure 5). Two mechanisms for the regeneration of I can be envisaged. They are, first, reaction of IO at the walls yielding I atoms and, second, a gas-phase reaction between IO and NO_3 regenerating I (a process which does not involve surfaces but is included here since it is kinetically similar to the heterogeneous regeneration of I from IO).

The first possibility can be analyzed by assuming that the two reactions

$$I + NO_3 \rightarrow IO + NO_2 \qquad (2)$$

$$IO + \text{wall} \rightarrow I + \text{wall} \qquad (18)$$

govern [I]. At the steady state reached at longer contact times

$$\frac{k_{18}}{k_2} = \frac{[NO]_3}{([I]_0/[I]_t)_{ss} - 1} \qquad \text{(ii)}$$

where $([I]_0/[I]_t)_{ss}$ is the ratio of the I atom signal in the absence and presence of NO_3 at long contact times. Values of $([I]_0/[I]_t)_{ss}$,

(55) Van den Bergh, H.; Troe, J. *J. Chem. Phys.* **1976**, *64*, 736.
(56) Laidler, K. J. *Chemical Kinetics*, 3rd ed.; Harper and Row: New York, 1987.
(57) Ip, J. K. K.; Burns, G. *J. Chem. Phys.* **1972**, *56*, 3155.
(58) Lilenfeld, H. V.; Bradburn, G. R. *J. Phys. Chem.* **1987**, *91*, 1981.
(59) Heard, A. C. D.Phil. Thesis, Oxford University, 1991.
(60) Walker, R. E. *Phys. Fluids* **1961**, *4*, 1211.

TABLE VI: Correction to k_2 for IO + Wall → I + Wall

10^{-12}[NO_3], molecules cm^{-3}	$[I]_{0,ss}/[I]_{t,ss}$	$10^{-10}k_{18}/k_2$, molecules cm^{-3}	$k_{18,fit}$, s^{-1}	$10^{10}k_{2,fit}$, cm^3 $molecule^{-1}$ s^{-1}	$10^{10}k_{2,expt}$, cm^3 $molecule^{-1}$ s^{-1}	α
0.9	12	8	25	3.7	4.1	0.83
0.6	7.4	8	45	6.1	5.8	1.18
1.0	13.5	7	40	5.4	4.0	1.06
1.2	15.6	8	30	4.1	4.0	1.35
2.0	33.1	6	35	4.7	4.0	1.03

[NO_3], and the corresponding values of k_{18}/k_2 calculated using eq ii are given in Table VI. The experimentally observed variations of $\ln\{[I]_0/[I]_t\}$ vs t were simulated by numerical integration of the coupled differential equations describing the concentration–time dependence of I; k_2 and k_{18} were varied according to the condition that $k_{18}/k_2 = 7.4 \times 10^{10}$ molecules cm^{-3} (the average of the values given in Table VI). The visual "best fit" values of $k_{18,fit}$ and $k_{2,fit}$ are shown in Table VI. The influence of reaction 18 on the initial slope, k_2', is represented by α, the ratio of the simulated and experimentally determined rate constants, $\alpha = k_{2,fit}/k_{2,expt}$ (where $k_{2,expt} = k_2'/[NO_3]$). Values of α and $k_{2,expt}$ are also given in Table VI. The average value of α is found to be 1.1; the variation in α probably arises from random scatter in the experimental data, and reaction of IO in process 18 will offset the measured decay in [I] by about 10%.

It should be noted that the ratio k_{18}/k_2 is reproducible for different experimental conditions. The excellent match between the predicted and experimental dependence of $\ln([I]_0/[I]_t)$ on t is illustrated in Figure 5. The solid line in the figure is that numerically simulated in the way just discussed. The required rate constant for loss of IO at the walls to generate I ranges from 25 to 45 s^{-1}. Other workers have reported values for

$$IO + \text{wall} \rightarrow \text{products} \qquad (19)$$

of 40[52] and 200 s^{-1}.[53] Loss of IO at the surface of the flow reactor might result in the formation of a deposit of formula I_xO_y. Stable oxides of iodine include I_2O_5 and I_4O_9.[61] Reaction of IO at the walls is therefore probably better represented by

$$IO + I_xO_y(s) \rightarrow I + I_xO_{y+1}(s) \qquad (18a)$$

The second hypothesis is that IO reacts with NO_3 to liberate I. The transformations involving I atoms would now be represented by the equations

$$I + NO_3 \rightarrow IO + NO_2 \qquad (2)$$

$$IO + NO_3 \rightarrow I + O_2 + NO_2 \qquad (20)$$

At the steady state

$$\frac{k_2}{k_{20}} = \left(\frac{[I]_0}{[I]_t}\right)_{ss} - 1 \qquad \text{(iii)}$$

Using the values of $([I]_0/[I]_t)_{ss}$ given in Table VI, we find that k_2/k_{20} = 14.6, 32.1, 12.5, 11, and 6.4 for the five runs analyzed. The poor reproducibility of the ratio of the rate constants for reactions 2 and 20 should be compared with the excellent reproducibility of the ratio k_{18}/k_2 just discussed. It appears that the homogeneous reaction between IO and NO_3 to give I atoms cannot be used to readily explain the formation of a steady state of I in the reaction system studied in this work.

We have shown in this section that the observed decay in [I] in the presence of NO_3 is unlikely to be influenced by homogeneous reactions other than reaction 2, that a change in k_w for I on addition of NO_3 to the flow reactor could contribute at most 15% to the observed decay, that heterogeneous reaction of IO at the walls to generate I is the most likely explanation for the apparent curvature in the pseudo-first-order plots obtained in this work, and further that reaction 18 could offset the observed decay in [I] by about 10%. However, the scatter in the correction factors α presented in Table VI is large enough that a further correction of 10% should be applied only with caution, and we consequently prefer to report a value for the second-order rate coefficient for reaction 2 of $k_2 = (4.5 \pm 1.9) \times 10^{10}$ cm^3 $molecule^{-1}$ s^{-1} and not to make corrections for heterogeneous processes.

(61) Greenwood, N. N.; Earnshaw, A. *Chemistry of the Elements*; Pergamon Press: Oxford, 1984.

TABLE VII: Rate Coefficients for Reactions between NO_3 and Halogen Atoms

reaction	k, cm^3 $molecule^{-1}$ s^{-1}	ref
$F + NO_3 \rightarrow FO + NO_2$	3.0×10^{-11}	13
	$>5 \times 10^{-11}$	14
	7×10^{-11}	15
$Cl + NO_3 \rightarrow ClO + NO_2$	$(7.6 \pm 1.1) \times 10^{-11}$	12
	$(2.7 \pm 1.0) \times 10^{-11}$	16
	$(5.5 \pm 2.0) \times 10^{-11}$	17
	$(2.6 \pm 0.5) \times 10^{-11}$	18
	$(4.3 \pm 1.3) \times 10^{-11}$	19
$Br + NO_3 \rightarrow BrO + NO_2$	$(1.6 \pm 0.5) \times 10^{-11}$	20
$I + NO_3 \rightarrow IO + NO_2$	$(4.5 \pm 1.2) \times 10^{-10}$	this work

4.2.3. Mechanism of the Reaction between NO_3 and I. The reaction of I with NO_3 to give IO and NO_2 is exothermic by 38 kJ mol^{-1} and is the most likely reaction pathway for the process. The explanation for the curvature observed in the pseudo-first-order plots for reaction 2 provides circumstantial evidence for the formation of IO in the reaction between I and NO_3.

The value for k_2 reported at the end of the last section can be compared with the hard-sphere collision frequency factor, Z'. We estimate values of the hard-sphere radii of I (3.93 Å) and NO_3 (3.97 Å) from published values[28] of the atomic volumes, V_b, of I, N, and O. On this basis, $Z' = 7.6 \times 10^{-10}$ cm^3 $molecule^{-1}$ s^{-1}. Thus, reaction between I and NO_3 occurs at about 60% of the collision rate.

4.2.4. A Comparison with Other Measurements of the Reactions of Halogen Atoms with NO_3. Lançar et al.[21] have provided the only other published information relevant to the reaction between I and NO_3. These workers measured the rate coefficient for the reaction between HI and NO_3

$$HI + NO_3 \rightarrow HNO_3 + I \qquad (21)$$

using a low-pressure discharge-flow technique, by monitoring the increase in EPR signal from iodine atoms formed in reaction 21. Lançar et al. measured the rate of loss of [NO_3] by mass spectrometry in the same system and found a good agreement between the loss in [NO_3] and the gain in [I], although the signal from NO_3 in the mass spectrometer was rather poor due to a large interference from the cracking ion of HNO_3 molecules. However, the observation is rather surprising if I reacts with NO_3 at anything like the rate that we have observed by direct methods in the present work, unless the same process operates to regenerate I in a similar way to that found in our experiments. Without detailed examination of the experimental data obtained by Lançar and coworkers, it is fruitless to speculate further on the origin of the apparently contrary observations from our work and theirs.

The reactions of NO_3 with the halogen atoms F, Cl, Br, and I can now be compared. The bimolecular rate coefficients for reactions of NO_3 with X are summarized in Table VII. It appears that, by analogy with the other reactions of halogen atoms with NO_3, the homogeneous reaction between I and NO_3 is expected to be rapid in the gas phase so long as the thermochemistry is favorable. However, that the rate coefficient approaches the gas-kinetic limit is somewhat surprising, especially if the apparent decrease in reactivity from Cl to Br is real. It may be that in the reaction with I there are special long-range interactions, and further investigation of the reaction is evidently warranted.

4.2.5. Tropospheric Chemistry of Iodine, NO_3, and Ozone. The reactions between I_2 or I and NO_3, discovered and quantified

during the course of this work, can only influence concentrations of O_3, NO_x, or iodine species when NO_3, I_2, and I are present simultaneously in significant amounts in the atmosphere. Iodine species exist in highest concentrations in air masses with a marine history, whereas $[NO_3]$ is greatest over continental areas, so that the reactions studied in this work are expected to be important in coastal regions only. As yet, the emissions of I_2, HOI, or I from the ocean surface believed to occur[4,62] are not well quantified and have not been included in tropospheric models. If the action of ozone at the sea surface does indeed release I_2 to the atmosphere, as suggested by Garland and Curtis,[4] then there is a nighttime source of I_2. The iodine either will react with NO_3

$$I_2 + NO_3 \rightarrow I + IONO_2 \quad (1a)$$

or will deposit on aerosols or the sea surface. For a typical concentration of NO_3 in the boundary layer of 2.5×10^7 molecules cm^{-3},[63] the atmospheric lifetime for removal of I_2 by reaction with NO_3 is about 7.5 h compared with lifetimes of 1 day for dry deposition and irreversible attachment to aerosol particles.[11] Thus, it appears that, during the night, the reaction between NO_3 and I_2 may be the dominant process for removal of I_2. However, the figures used for the rate of deposition must be treated with caution, as the chemistry of iodine on or in aerosols is poorly defined,[10] and it is possible that I_2 is *released* by processes such as

$$2IO_3^- + 5H_2O_2 + 2H^+ \rightarrow I_2 + 5O_2 + 6H_2O \quad (22)$$

occurring in cloud droplets.[64]

Reaction 1a constitutes a nighttime source of iodine atoms and, therefore, a route for the consumption of O_3 via the reaction sequence

$$I_2 + NO_3 \rightarrow I + IONO_2 \quad (1a)$$

$$I + O_3 \rightarrow IO + O_2 \quad (23)$$

The rate of reaction between I and NO_3 ($k_2 = 4.5 \times 10^{-10}$ cm^3 $molecule^{-1}$ s^{-1}) can be used to calculate a lifetime for removal of I (again using $[NO_3] = 2.5 \times 10^7$ molecules cm^{-3}) of 100 s, compared with a lifetime for removal against reaction with O_3 (typical concentration of 6.25×10^{11} molecules cm^{-3} [63]) of 1.6 s, so that, as for the daytime, I is mainly removed by reaction with ozone. Our new work thus indicates that the main influence of NO_3 on atmospheric iodine chemistry is likely to be through the reaction with I_2 rather than the interactions with atomic iodine. The consequences of reaction 1 are loss of I_2 and a possible nighttime consumption of O_3.

Acknowledgment. A.C.H. thanks the Gassiot Committee of the Meterological Office for a research training studentship under the auspices of which this research was conducted. We also thank Drs. P. Biggs and C. E. Canosa-Mas for practical and other assistance and Mr. P. S. Monks for his computer expertise.

(62) Thompson, A. M.; Zafiriou, O. C. *J. Geophys. Res.* **1983**, *88*, 6696.
(63) Brauers, T.; Platt, U.; Dorn, H.-P.; Neuroth, R. In *Physico-chemical Behaviour of Atmospheric Pollutants*; Restelli, G., Angeletti, G., Eds.; Kluwer Academic Publishers: Dordrecht, 1990; pp 237-242.
(64) Furrows, S. D.; Noyes, R. M. *J. Am. Chem. Soc.* **1982**, *104*, 45.

A Nanosecond Laser Flash Photolysis Study of Intramicellar Reactions in the Erythrosin B/CTAB Aqueous System

Lucia Flamigni

Istituto F.R.A.E.-C.N.R., Via de' Castagnoli, 1, 40126 Bologna, Italy *(Received: October 23, 1991; In Final Form: December 30, 1991)*

Both "fast", occurring within 1 μs after excitation, and "slow" reactions, occurring in the hundreds of microseconds time scale, were observed following erythrosin B triplet formation in the cationic micellar system cetyltrimethylammonium bromide (CTAB). The "fast" events are shown to occur in multiply occupied micelles and are assigned to bimolecular reactions. The "slow" ones, which have not been studied in detail, are due to first-order deactivation processes of the triplet occurring in singly occupied micelles. The effects of the excitation intensity and occupancy on the fast triplet decay, radical formation, and subsequent geminate recombination have been studied. The triplet disappears with observed rate constants ranging from 5.5×10^6 to 3.6×10^6 s^{-1} while the formation of radicals has rate constants varying from 3.3×10^7 to 9.1×10^6 s^{-1}. Both in triplet decay and in radical formation the increase in rates occurs by increasing the excitation energy and occupancy. The identification of the precursor(s) of radicals is discussed. The geminal radical recombination has a rate constant of 2.1×10^6 s^{-1}.

Introduction

Transient intermediates obtained upon light absorption in xanthene dyes in homogeneous solutions have been the object of intense investigations since the early days of flash photolysis.[1-10] Time-resolved luminescence studies on these systems appeared later as a consequence of the short lifetime of the singlet state, requiring subnanosecond resolution.[11-13]

Because of the wide applications of these dyes in several fields (solar energy conversion, laser dyes, biological markers, singlet oxygen photosensitizers, photoinitiators of polymerization, etc.), the interest in such compounds is still very lively. More recently, studies aimed at understanding the behavior of such dyes in heterogeneous systems like micelles,[14-25] polymers,[26-28] vesicles,[29]

(1) Kato, S.; Koizumi, M. *Nature* **1959**, *184*, 1620.
(2) Grossweiner, L. I.; Zwicker, E. F. *J. Chem. Phys.* **1959**, *31*, 1141.
(3) Lindqvist, L. *Ark. Kemi* **1960**, *16*, 79.
(4) Grossweiner, L. I.; Zwicker, E. F. *J. Chem. Phys.* **1961**, *34*, 1411.
(5) Zwicker, E. F.; Grossweiner, L. I. *J. Chem. Phys.* **1963**, *67*, 549.
(6) Lindqvist, L. *J. Phys. Chem.* **1963**, *67*, 1707.
(7) Kasche, V.; Lindqvist, L. *J. Phys. Chem.* **1964**, *68*, 817.
(8) Kasche, V.; Lindqvist, L. *Photochem. Photobiol.* **1965**, *4*, 923.
(9) Bowers, P. G.; Porter, G. *Proc. R. Soc. London, A* **1967**, *299*, 348.
(10) Nemoto, N.; Kokubun, H.; Koizumi, M. *Bull. Chem. Soc. Jpn.* **1969**, *42*, 1223. Nemoto, N.; Kokubun, H.; Koizumi, M. *Bull. Chem. Soc. Jpn.* **1969**, *42*, 2464.
(11) Porter, G.; Reid, E. S.; Tredwell, J. *Chem. Phys. Lett.* **1974**, *29*, 469.
(12) Fleming, G. R.; Knight, A. W. E.; Morris, J. M.; Morrison, R. J. S.; Robinson, G. W. *J. Am. Chem. Soc.* **1977**, *99*, 43.
(13) Cramer, L. E.; Spears, K. G. *J. Am. Chem. Soc.* **1978**, *100*, 221.
(14) Rodgers, M. A. J. *Chem. Phys. Lett.* **1981**, *78*, 509.
(15) Rodgers, M. A. J. *J. Phys. Chem.* **1981**, *85*, 3372.
(16) Seret, A.; Gandin, E.; Van de Vorst, A. *Chem. Phys. Lett.* **1987**, *135*, 427.
(17) Seret, A.; Gandin, E.; Van de Vorst, A. *J. Photochem.* **1987**, *38*, 145.

0022-3654/92/2096-3331$03.00/0